Available online at www.sciencedirect.com

ScienceDirect

journal homepage: http://www.elsevier.com/locate/rpor

Original research article

Dosimetric and Monte Carlo verification of jaws-only IMRT plans calculated by the Collapsed Cone Convolution algorithm for head and neck cancers

Duong Thanh Tai[a,b,d,*], *Luong Thi Oanh*[d,b], *Nguyen Dong Son*[c], *Truong Thi Hong Loan*[b], *James C.L. Chow*[e,f]

[a] *Department of Radiation Oncology, Dong Nai General Hospital, Bien Hoa 810000, Viet Nam*
[b] *Faculty of Physics & Engineering Physics, VNUHCM-University of Science, Ho Chi Minh 749000, Viet Nam*
[c] *Chi Anh Medical Technology Co., Ltd., Ho Chi Minh 717066, Viet Nam*
[d] *Faculty of Medicine, Nguyen Tat Thanh University, Ho Chi Minh 702000, Viet Nam*
[e] *Department of Radiation Oncology, University of Toronto, Toronto M5T 1P5, Canada*
[f] *Princess Margaret Cancer Centre, University Health Network, Toronto M5G 1Z5, Canada*

ARTICLE INFO

Article history:
Received 12 April 2018
Received in revised form
24 July 2018
Accepted 10 November 2018
Available online 28 November 2018

Keywords:
Intensity-modulated radiation therapy (IMRT)
Jaws-only IMRT (JO-IMRT)
Quality assurance (QA)
Monte Carlo simulation (MC)
CERR
DOSCTP

ABSTRACT

Aim: The aim of this study is to verify the Prowess Panther jaws-only intensity modulated radiation therapy (JO-IMRT) treatment planning (TP) by comparing the TP dose distributions for head-and-neck (H&N) cancer with the ones simulated by Monte Carlo (MC).
Background: To date, dose distributions planned using JO-IMRT for H&N patients were found superior to the corresponding three-dimensional conformal radiotherapy (3D-CRT) plans. Dosimetry of the JO-IMRT plans were also experimentally verified using an ionization chamber, MapCHECK 2, and Octavius 4D and good agreements were shown.
Materials and methods: Dose distributions of 15 JO-IMRT plans of nasopharyngeal patients were recalculated using the EGSnrc Monte Carlo code. The clinical photon beams were simulated using the BEAMnrc. The absorbed dose to patients treated by fixed-field IMRT was computed using the DOSXYZnrc. The simulated dose distributions were then compared with the ones calculated by the Collapsed Cone Convolution (CCC) algorithm on the TPS, using the relative dose error comparison and the gamma index using global methods implemented in PTW-VeriSoft with 3%/3 mm, 2%/2 mm, 1%/1 mm criteria.
Results: There is a good agreement between the MC and TPS dose. The average gamma passing rates were 93.3 ± 3.1%, 92.8 ± 3.2%, 92.4 ± 3.4% based on the 3%/3 mm, 2%/2 mm, 1%/1 mm criteria, respectively.

* *Corresponding author at*: Department of Radiation Oncology, Dong Nai General Hospital, Bien Hoa 810000, Viet Nam.
E-mail address: thanhtai_phys@yahoo.com (D.T. Tai).
https://doi.org/10.1016/j.rpor.2018.11.004

Conclusions: According to the results, it is concluded that the CCC algorithm was adequate for most of the IMRT H&N cases where the target was not immediately adjacent to the critical structures.

1. Background

Jaws-only intensity modulated radiation therapy (JO-IMRT) is a technique that uses the integrated jaws of the linear accelerator (LINAC) to create complex intensity patterns comparable to multileaf collimator (MLC)-based IMRT.[1] The main advantage of JO-IMRT is the lack of additional complexity and expense of an MLC,[2] while allowing IMRT to be achieved at lower cost. In addition, JO-IMRT can be an alternative technique which could be applied for any exceptional situations, for example, in the case of a failure of the MLC system. Moreover, the advantage of the JO-IMRT application comes from the more profitable treatment plans in many cases which is confirmed by a series of recent studies.[4–6] The presented work can also be interesting for manufacturers of treatment planning systems. *First*, we tested the capabilities of creating dose distributions with JO-IMRT. Our results showed that JO-IMRT gives better dose distributions than 3D-CRT.[4,5] *In the second study*, we used an ionization chamber, MapCHECK 2, and Octavius 4D, to verify the dose distributions planned for H&N patients. The results show a good agreement between measured and calculated dose: the JO-IMRT plans for H&N patients were accurate and suitable for treatment delivery.[6] *In the present study*, we verify the JO-IMRT dose distributions using the Monte Carlo simulation (MC).

The MC code used for this work is the EGSnrc-based BEAMnrc and DOSXYZnrc, a strong tool which has been used by many authors to verify IMRT TPS dose calculations.[7–12] Ma et al. used Monte Carlo method to verify the accuracy of Corvus TPS (*Corvus, Nomos Corp., Sewickley, PA*) for two patient plans. The dose differences between Monte Carlo and TPS are found to be 5% for target structures and over 20% for critical structures.[7] Francescon et al. performed comparison of dose distributions calculated by Pinnacle[3] TPS (*Philips Medical Systems, Milpitas, CA*) and EGS4 for two plans. They showed that the discrepancies of dose at isocenter was 2.1% for a prostate plan and 2.9% for a head-and-neck plan. They also used dose-volume histogram (DVH) data for comparisons. The deviation was about 6%.[9] Leal et al. investigated the use of MC to verify the step-and-shoot IMRT plans using the Plato TPS (*Veenendall, Netherlands*) and compared with EGS4-based calculations and film dosimetry for 3 cases. The major differences between MC and TPS were found in media with high heterogeneity such as head-and-neck, where contain air–tissue–bone interfaces. On the other hand, the minor differences were found in homogeneous regions, such as the prostate.[10]

While MC has been extensively used to verify TPS dose calculation accuracy, MC verification of JO-IMRT plans has yet to be conducted. In this report, we present the results of using MC for verification of the JO-IMRT dose distributions from a Prowess Panther TPS for H&N cancer. For that purpose, dose distributions of 15 JO-IMRT plans of nasopharyngeal patients were recalculated using the EGSnrc Monte Carlo code. The photon beams from a Siemens Primus LINAC were simulated using the BEAMnrc.[13,14]

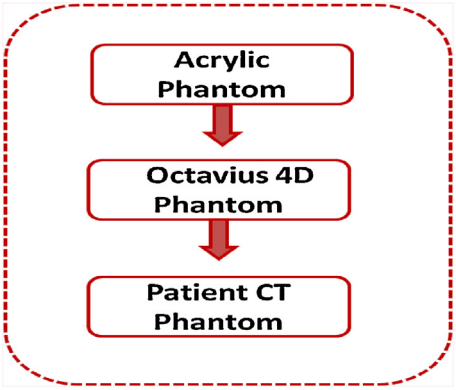

Fig. 1 – Flowchart of the main process.

2. Aim

The aim of this study is to verify the JO-IMRT treatment planning for H&N cancer by comparing the TPS dose distributions with the ones simulated by MC.

3. Materials and methods

This study is comprised of 3 steps (Fig. 1). These steps pose a range of simulation problems requiring dose calculations/measurements using phantom models of varying complexity. Step 1 assesses the simplest case on acrylic phantoms including 20 slabs (30 cm × 30 cm × 1 cm) densities of 1.1 g/cm^3. Step 2 ensures a more complicated case on Octavius 4D phantom. Step 3 is done with a clinical treatment case.

3.1. *Treatment planning*

In the first step, to evaluate the accuracy of dose calculation in the interface region near air cavities within an otherwise homogeneous acrylic phantom, model single beams irradiate solid acrylic phantoms (30 cm × 30 cm × 20 cm) with and without an air cavity (15 cm × 4 cm × 4 cm) which is 2.5 cm away from the anterior surface of the phantom. The dose distributions were measured, calculated by the TPS and simulated with the EGSnrc.[15]

In the second step, the JO-IMRT plans for nasopharyngeal patients, generated by Prowess Panther v4.6, were transferred

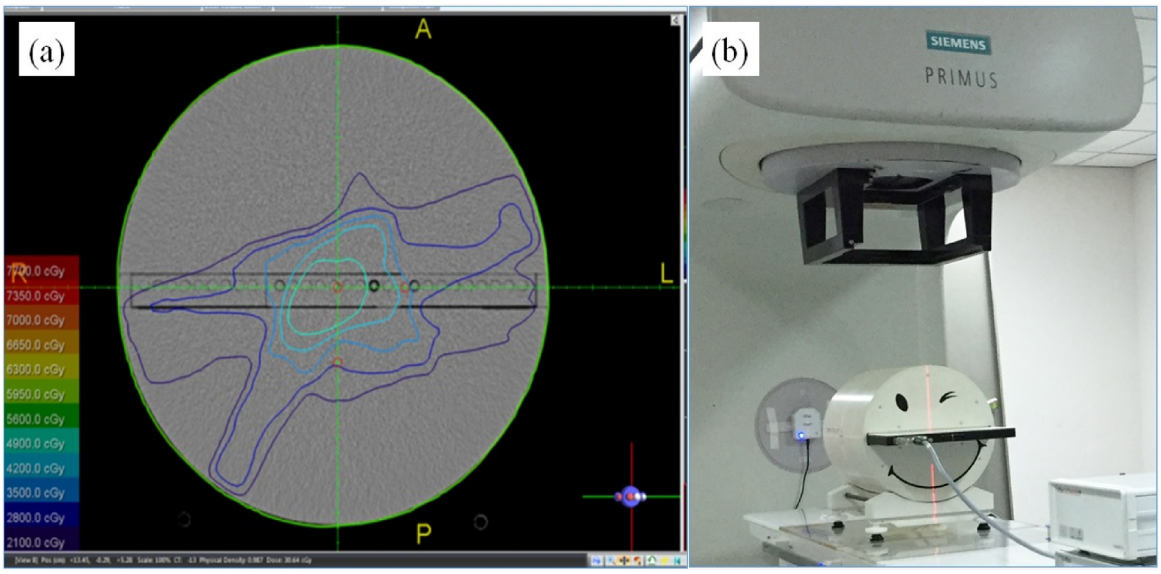

Fig. 2 – Dose distributions (a) of the Octavius phantom measured according to the set up as shown in (b).

to an Octavius 4D phantom, which comprises five main components: a rotation unit, 2D-array detector plate, inclinometer, electrometer, and control unit. The dose distributions in this phantom were calculated by the TPS (Fig. 2a), simulated with EGSnrc and measured with the detectors of the Octavius phantom (Fig. 2b), which was set up according to our previous work[6]: the cylindrical rotation unit was fixed horizontally on the treatment table, its center positioned at the isocenter. The data acquisition measurement was processed inside a 2D-array detector plate, which was inserted into the rotation unit. The inclinometer was pinned to the LINAC gantry in order to measure and transmit the real-time gantry angle to the control unit via Bluetooth signals. According to these gantry angle data, the control unit operated the rotation unit in order to synchronize the rotation between gantry and the rotation unit. In this situation the detector array is always perpendicular to the radiation beam axis.

In the third step, the dose distribution in nasopharyngeal patients treated by JO-IMRT was simulated and compared with the one calculated by the TPS. The Panther TPS with a Collapsed Cone Convolution (CCC) algorithm was used for calculation and optimization of isodoses for JO-IMRT plans. All plans were delivered using a step-and-shoot technique on a Siemens Primus with 6 MV photon beams. The JO-IMRT plans were generated by Prowess Panther v4.6. For each plan, seven beams at angles of 0, 50, 100, 150, 200, 250, and 300 degrees were employed with 7 segments per beam. So, there were 49 segments in total. The Panther's Collapsed Cone Convolution Superposition algorithm was used to calculate dose distributions with a 3 mm × 3 mm × 3 mm dose grid.

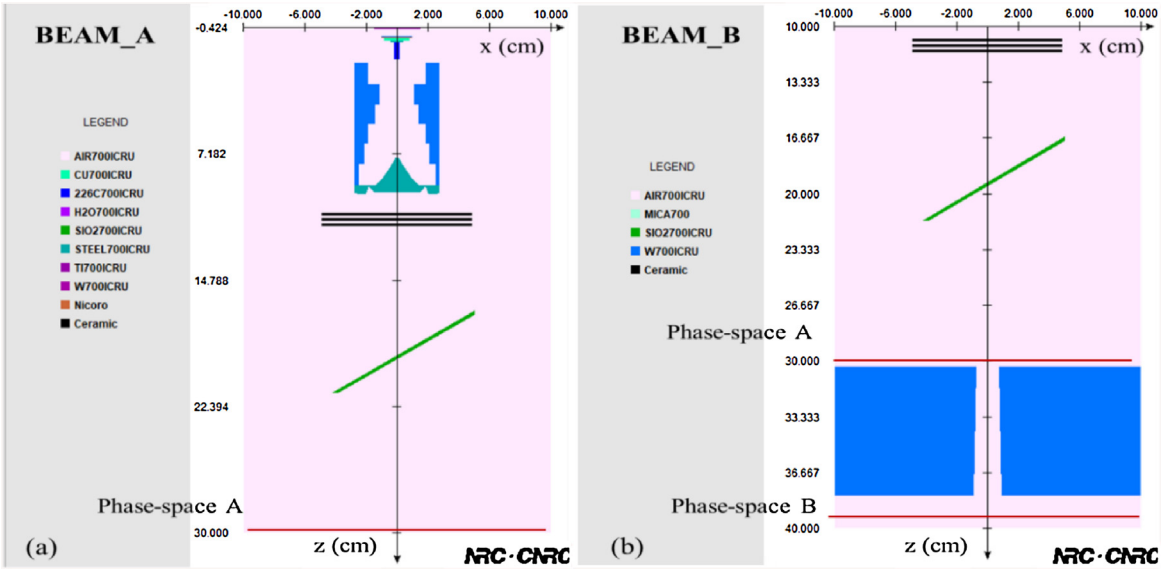

Fig. 3 – Two-step simulation of the LINAC regarding BEAM A (a) and BEAM B (b).

3.2. *The Monte Carlo simulation*

The BEAMnrc was used to simulate 6 MV photon beams produced by a Siemens Primus LINAC.[13,14] The material and geometric description of the head of LINAC was provided by the manufacturer. To reduce the computing time and facilitate dose calculations, the photon beam simulation of the LINAC was carried out in two separated steps (BEAM A and BEAM B as shown in Fig. 3) as suggested by Popescu et al.[16,17]

In the first step of BEAM A (Fig. 3a), the component modules from the beam source to the jaw (including exit window, target, primary collimator, flattening fllters, ion chambers, and mirror) were simulated. The output of BEAM A contained the phase-space data just below the mirror and was used as a source for the BEAM B simulation in the second step. The phase-space A was simulated for various fields of the 6 MV photon beams. The source routine, ISOURC = 19, was used in BEAM A. Two simulation parameters of the incident electron beam were determined in a previous work[18]: mean electron beam energy of 6.04 MeV and full width at half maximum (FWHM) of 1.2 mm in the X and Y directions. It is because the field size of the JO-IMRT plan is not greater than 10 cm × 10 cm. For the initial electron beam parameters above, the result also gave an excellent agreement between simulation and measurement for the percentage depth dose (PDD) and the off-center ratios (OCR) regarding various field sizes (from 3 cm × 3 cm to 10 cm × 10 cm) and different depths.

In the second step of BEAM B (Fig. 3b), including the internal ionization chambers, mirror, jaws, and reticle are then simulated. The output of BEAM B contained the phase-space B data, which were scored below the jaws for every beam segment and used as an input for the DOSXYZnrc. The DOSXYZnrc was used to calculate the dose distributions for patients (as CT images) who were treated by fixed-field IMRT.[19]

Because of the limited support in DOSXYZnrc regarding a CT image set, a graphical user interface (GUI) called the DOSCTP,[20,21] was used for calculating the 3D dose distribution. The *.egsphant file which was used as an input of the DOSCTP was created from the CT image set by the CTCREATE.

The EGSnrc transport parameters were set to AP = PCUT = 0.010 MeV and AE = ECUT = 0.700 MeV, where AP is the low-energy threshold for the production of secondary bremsstrahlung photons, AE is that for knock-on electrons, PCUT and ECUT are the global cutoff energies for photon and electron transport, respectively.[14,15,17,19] The variance reduction technique of directional bremsstrahlung splitting (DBS) was used to improve the computational efficiency. A total of 2×10^9 initial particle histories were simulated.

3.3. *Dose measurement*

The absolute dose for a field size of 10 cm × 10 cm was measured at multiple depths in a solid acrylic phantom (30 cm × 30 cm × 20 cm) using an aluminum electrode Farmer-type chamber (FC65-P) with a cavity length of 23.1 mm, diameter of 6.2 mm, volume of 0.65 cm^3, and a wall thickness of 0.057 g/cm^2 (IBA Dosimetry, Germany).[22] The dose distribution was measured using an Octavius 4D 1500 (PTW, Freiburg, Germany).

3.4. *Data analysis methods and evaluation criteria*

In order to compare MC simulation with TPS calculation and measurement, the absolute dose, isodose distributions, DVH, and gamma index were used. Fig. 4 shows the main process of comparing MC and TPS. The process begins with exporting a DICOM dataset from Panther TPS. The dataset includes a plan file and dose files containing the dose distribution in a patient. The 3ddose file from DOSCTP was converted to RTdose.*dcm by CERR (a computational environment for

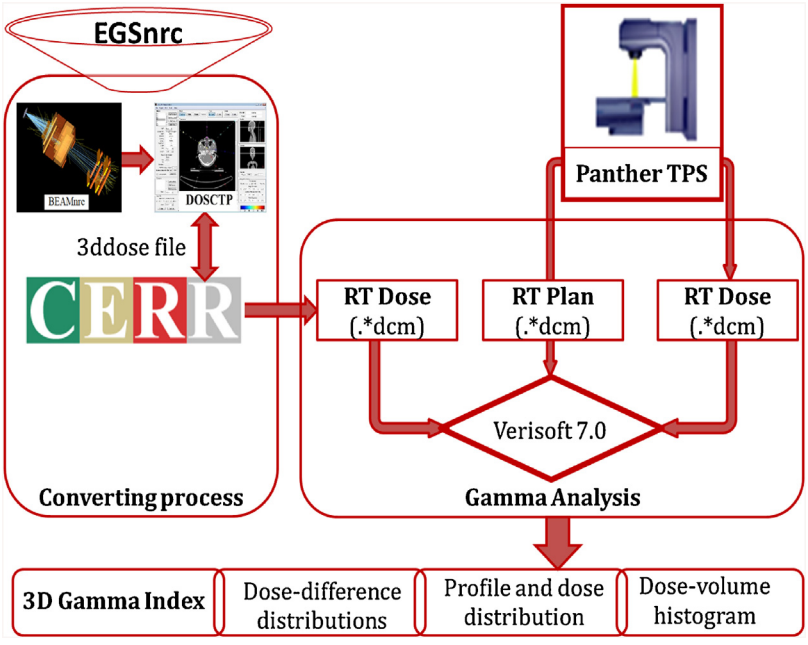

Fig. 4 – Flowchart of the main process of comparison MC and TPS.

radiotherapy research) which is written using MATLAB.[23] This RTdose.*dcm file can be imported into Panther TPS.

After the DICOM datasets from MC and TPS have been exported, the process of comparison was performed using VeriSoft 7.0 (PTW, Freiburg, Germany) for comparing gamma index with 3%/3 mm pass criteria and threshold of 10% of maximum dose and CERR/TPS for isodose distributions, DVH.

4. Results

4.1. *Results of simulation on the solid acrylic plate phantom*

A comparison of dose distributions in the acrylic phantom simulated by the EGSnrc and calculated by Panther TPS for a beam of field size 10 cm × 10 cm and 90 cm source-to-surface distance (SSD) are shown in Fig. 5. The pass rates with gamma evaluation of 3%/3 mm, 2%/2 mm, 1%/1 mm and 10% threshold of maximum dose were 98.7%, 96.4% and 94.2%, respectively. The profile (Fig. 5a) and PDD (Fig. 5b) showed a good agreement between MC and TPS. Furthermore, the gamma values are low and almost all points are smaller than 0.2 (Fig. 5c). Fig. 5d shows the gamma distribution map (Green 90%–100%, Yellow 75%–90%, Red 0%–75%).

To verify the accuracy of simulation using BEAMnrc/DOSXYZnrc code, the central axis depth doses of 1.5, 2.5, 3.5, 4.5, 5.5, 6.5, 7.5, 8.5, and 10 cm were compared. The results are presented in Fig. 6. The error bars represent experimental uncertainty of ±3%.

A 4.0 cm thick air cavity placed at 2.5 cm depth is inserted into the same phantom using a function for creating an air cavity in the Prowess Panther TPS. We calculated the PDDs using MC and CCC algorithms for FS of 1 cm × 1 cm, 3 cm × 3 cm, and 5 cm × 5 cm. Our results of MC simulation (Fig. 7) showed good consistence with those of Navin Singh et al. (2018).[24]

Fig. 8 shows the comparison of the PDD received from CCC calculation and MC simulation for the field size of 1 cm × 1 cm. We observed that the CCC algorithm of Prowess Panther TPS is in a good agreement with MC.

4.2. *Verification of the JO-IMRT plan in Octavius 4D 1500*

The gamma index using a variety of criteria (3%/3 mm, 2%/2 mm, 1%/1 mm) between the MC and TPS is 96.3%, 95.8%, 95.4%. The profiles in the anterior posterior direction (Fig. 9a) and isodoses (Fig. 9b) calculated by the TPS and MC for a JO-IMRT plan delivered to an Octavius phantom showed a good agreement. The gamma histogram (Fig. 9c) shows the numbers of voxels falling into the category of different gamma values. Most of the voxels fall into the 0–0.2 gamma value category. The passed and failed points (Fig. 9d) are shown in green and red, respectively.

The gamma passing rates (3%/3 mm, 2%/2 mm, 1%/1 mm) between the MC and measurement is 93.9%, 93.4%, 93.1%. The simulated and measured profiles (Fig. 10a) and isodoses (Fig. 10b) for the JO-IMRT plan in Octavius phantom showed good agreement. The gamma histogram (Fig. 10c) shows that most of voxels fall into the 0–0.2 gamma value. The green and

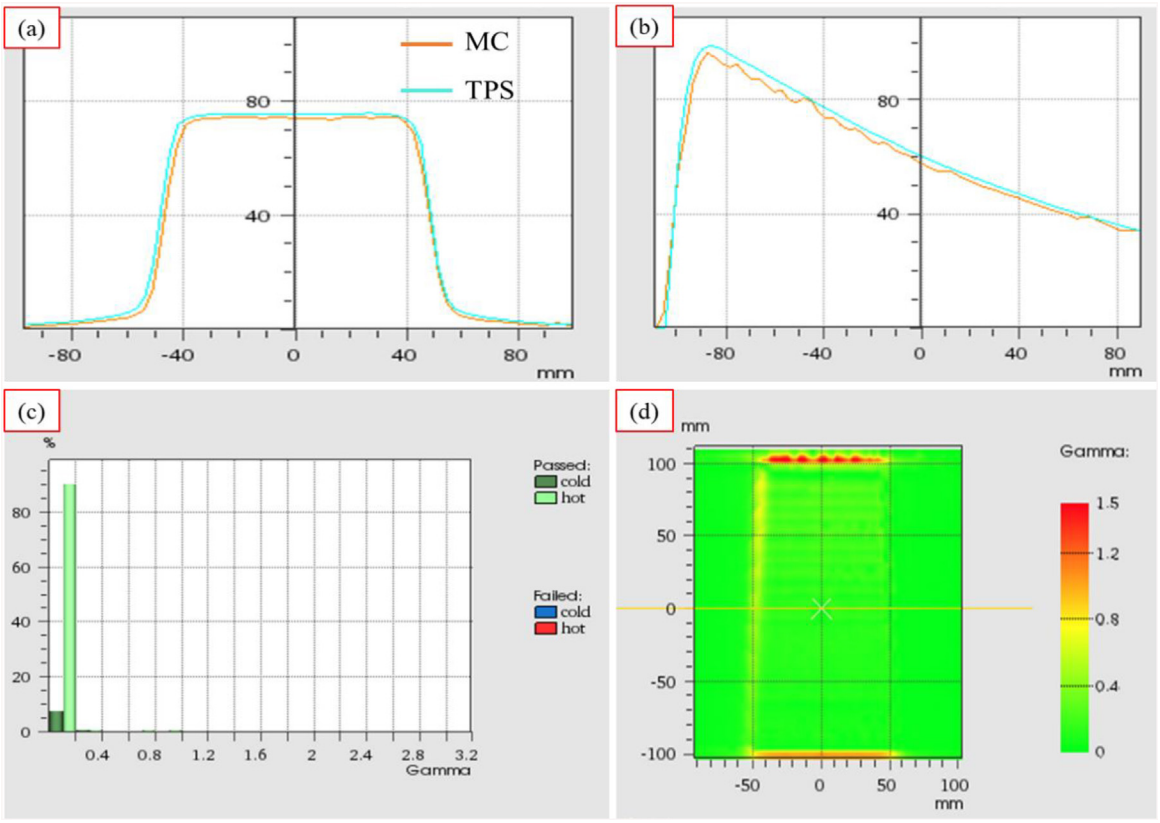

Fig. 5 – Comparison between MC simulation and TPS calculation for a single beam.

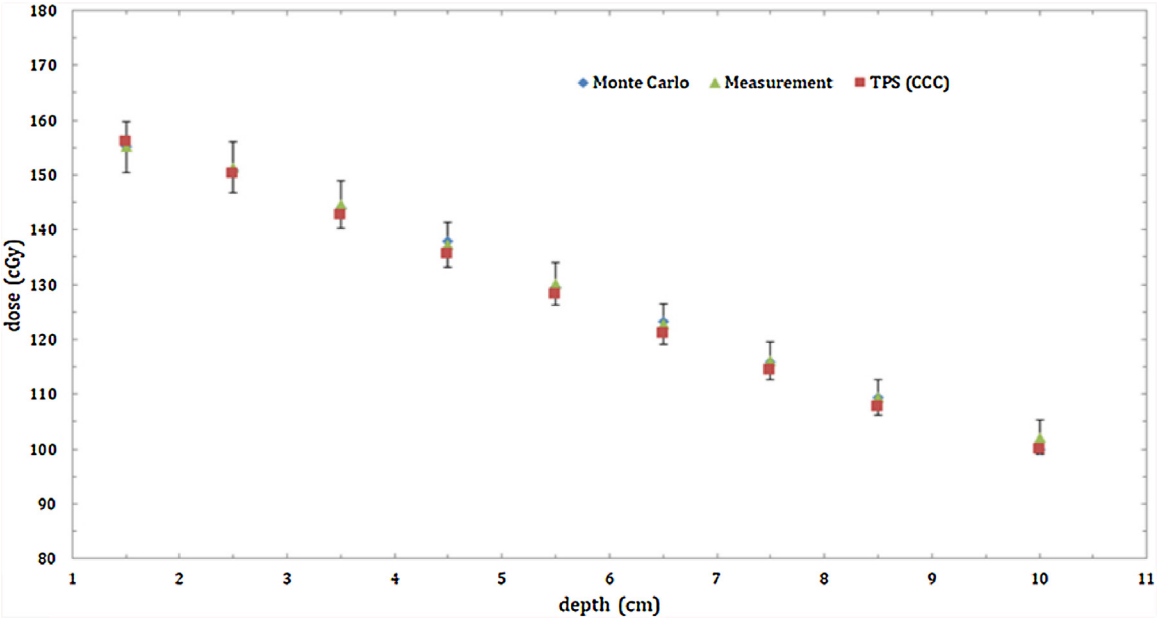

Fig. 6 – Comparison of absolute dose calculated by TPS and MC and from measurement.

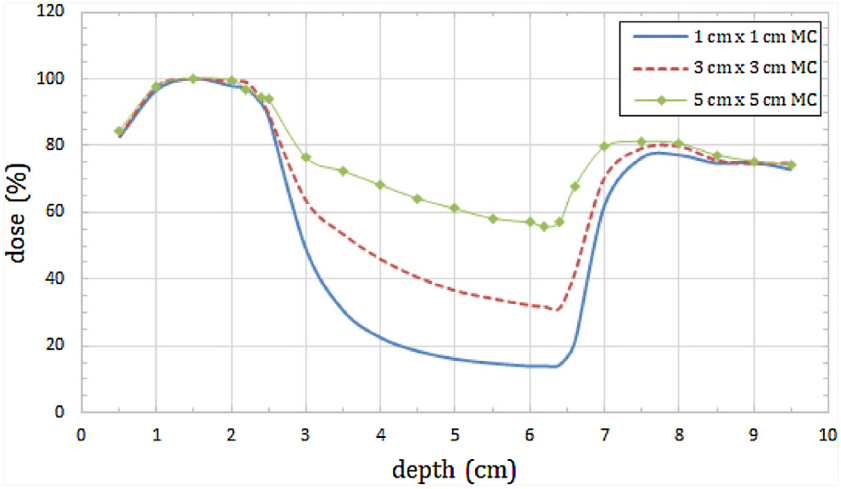

Fig. 7 – MC simulation results for the PDD with 4 cm air cavity placed at 2.5 cm depth.

red color in the gamma map (Fig. 10d) represent the passed and failed points, respectively.

4.3. *Verification of the JO-IMRT plan in head-and-neck cancer*

Before simulating the clinical JO-IMRT plans, we examined a simple small segment of 3 cm × 3 cm.

The result is shown in Fig. 11. The gamma index pass rate for this case was 100% with 3%/3 mm 2%/2 mm, 1%/1 mm criteria.

Fig. 12 shows the comparison of MC and TPS for an example treatment case. The profiles (Fig. 12a) and isodoses (Fig. 12b) between TPS and MC for plans of nasopharyngeal patients showed a good agreement. The gamma histogram of the comparison of dose distribution in volume (Fig. 12c) and gamma map (Fig. 12d) show a gamma value <1 are dominant.

Next, we compared the dose distributions calculated by the MC and the CCC algorithm for 15 JO-IMRT plans of nasopharyngeal patients. In general, the average gamma index of 15 JO-IMRT plans for the comparison of TPS and MC were 93.3 ± 3.1%, 92.8 ± 3.2%, 92.4 ± 3.4% based on 3%/3 mm; 2%/2 mm, 1%/1 mm criteria, respectively. The gamma pass rate decreased when the gamma criteria changed from 3%/3 mm to 1%/1 mm but the gamma pass rate for all the plans in this study was greater than 90% as acceptable in our hospital. The CT data, structures, and dose distribution from MC and TPS were then imported to the CERR and used in generating DVH.

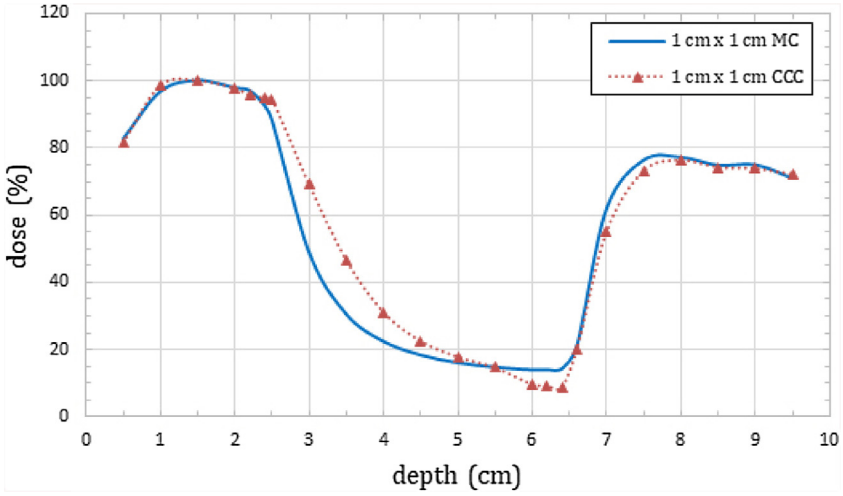

Fig. 8 – The percentage depth dose for 1 cm × 1 cm field size with 4 cm air cavity.

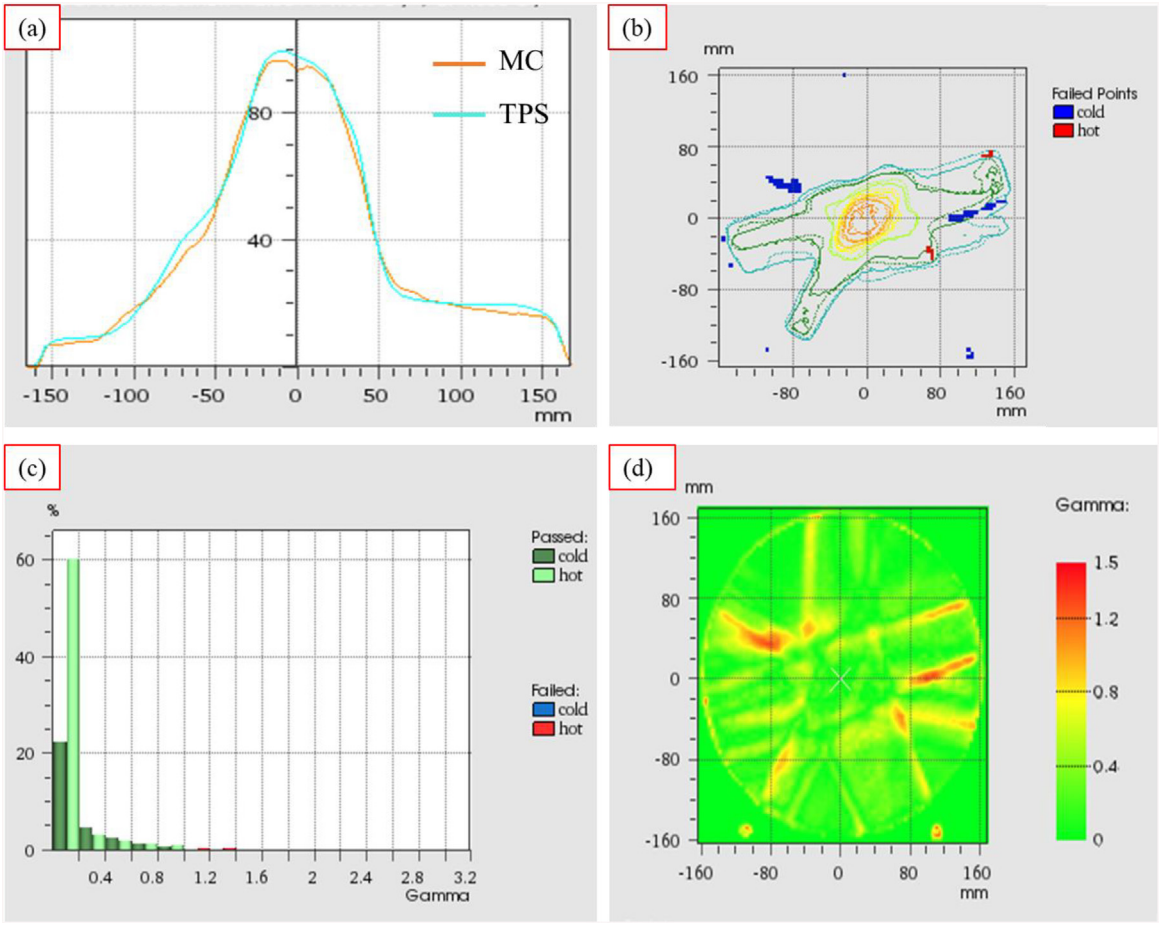

Fig. 9 – Comparison between MC simulation and TPS for JO-IMRT plan.

Fig. 13 demonstrates DVH of a sample plan for the PTV (red), parotid glands (green), and spinal cord (magenta). It can be seen that the maximum dose in the PTV agreed well between the TPS and the MC but the mean MC dose was lower than the TPS predicted dose.

The difference in the max dose to the spinal cord between the TPS (46.3 Gy) and the MC (53.1 Gy) was about 12.8%. This finding is in agreement with Ma's (2000) findings which showed the differences of 20%.[7] MC predicts about a 4.2% higher mean dose to the parotid glands as compared to TPS. This also accords with Sakthi's (2006) observations.[12]

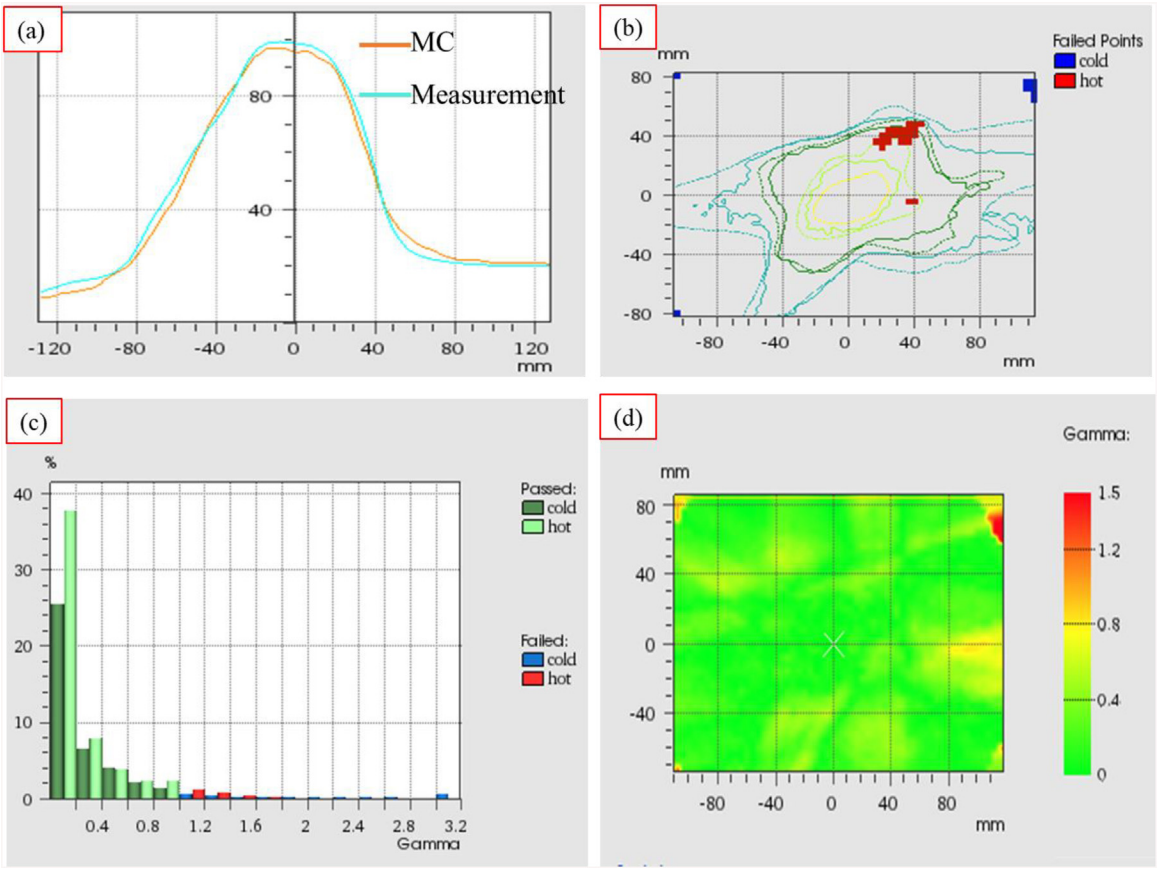

Fig. 10 – Comparison between MC simulation and Octavius 4D measurements.

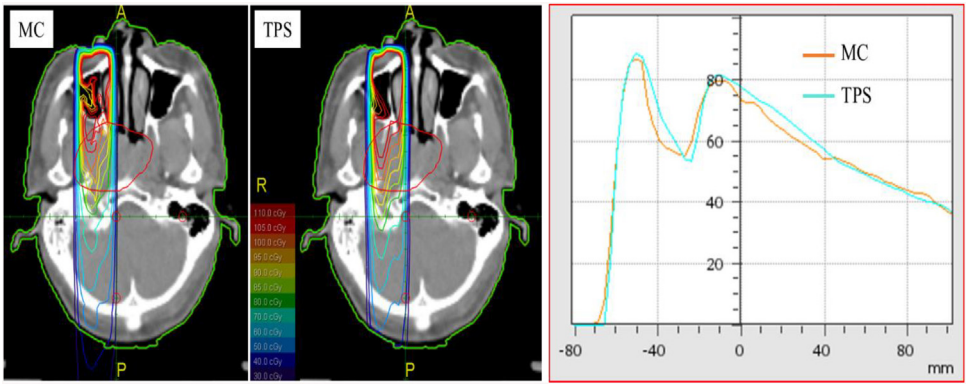

Fig. 11 – Dose distribution comparison between TPS and MC simulation for a single segment.

5. Discussion

As shown in Fig. 6, a good agreement between the experimental measurements, the TPS and Monte Carlo simulation of PDD curves along the central beam axis was achieved. Since the JO-IMRT techniques typically employ combinations of multiple small radiation segment of varying intensities to deliver highly conformal radiation therapy, the use of small segments in this techniques may therefore result in the inaccuracy of calculation of absorbed dose within an air cavity region. This work performed MC simulations for a small field size from 1 cm × 1 cm to 5 cm × 5 cm to investigate the effect of dose reduction near an air cavity. Fig. 7 shows MC simulation for PDDs of 1 cm × 1 cm, 3 cm × 3 cm, 5 cm × 5 cm. It is encouraging to compare this figure with that found by Navin Singh et al.[24] Fig. 8 shows that the PDDs obtained using MC simulations for 1 cm × 1 cm are very close to the PDDs obtained by TPS in the air cavity. The dose was reduced at the interface region near the air cavity (the dose re-buildup region). The magnitude of dose reduction decreases with the increase in the field size of beams.[24] Hideharu et al.[25] and Bergman et al.[17] reported this problem as encountered when the tissue is inhomogeneous. Our results are consistent with these findings.

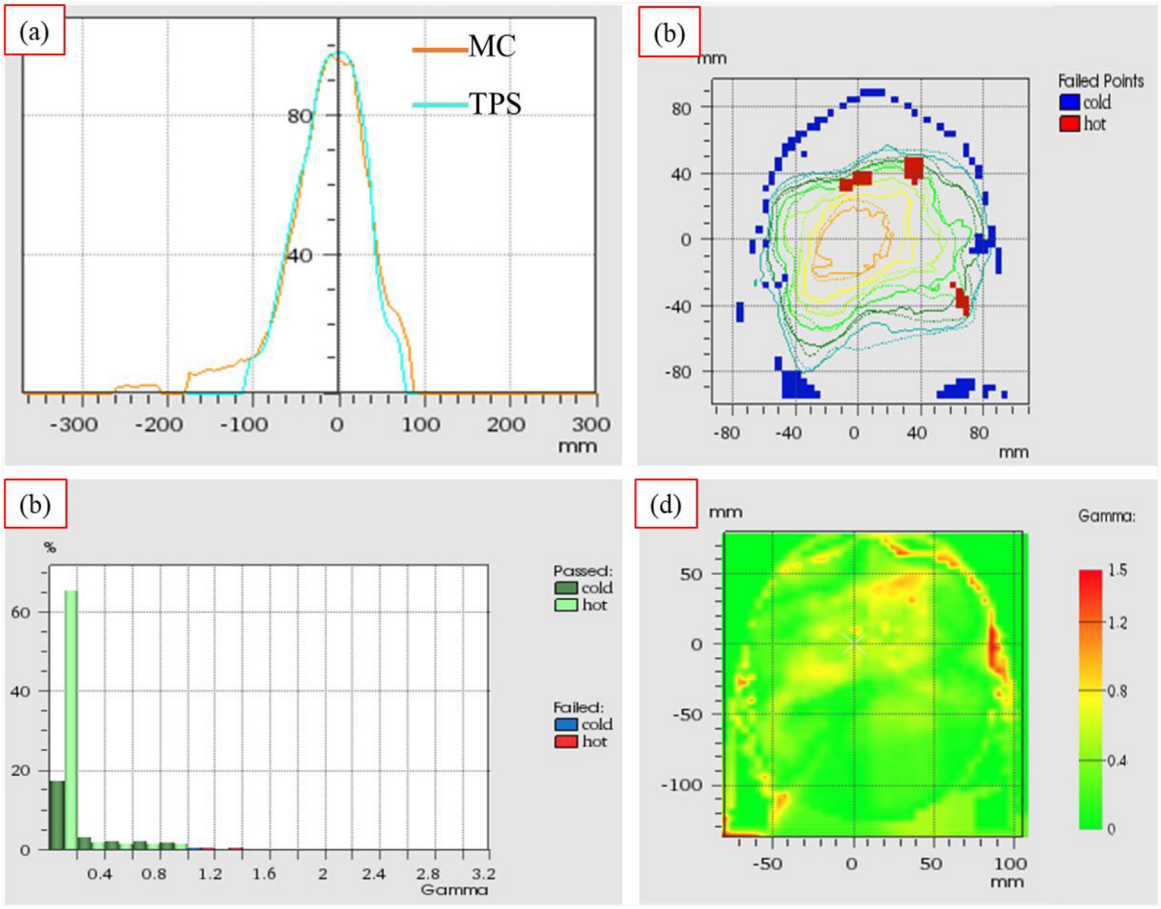

Fig. 12 – Comparison of dose distribution in MC calculation and TPS.

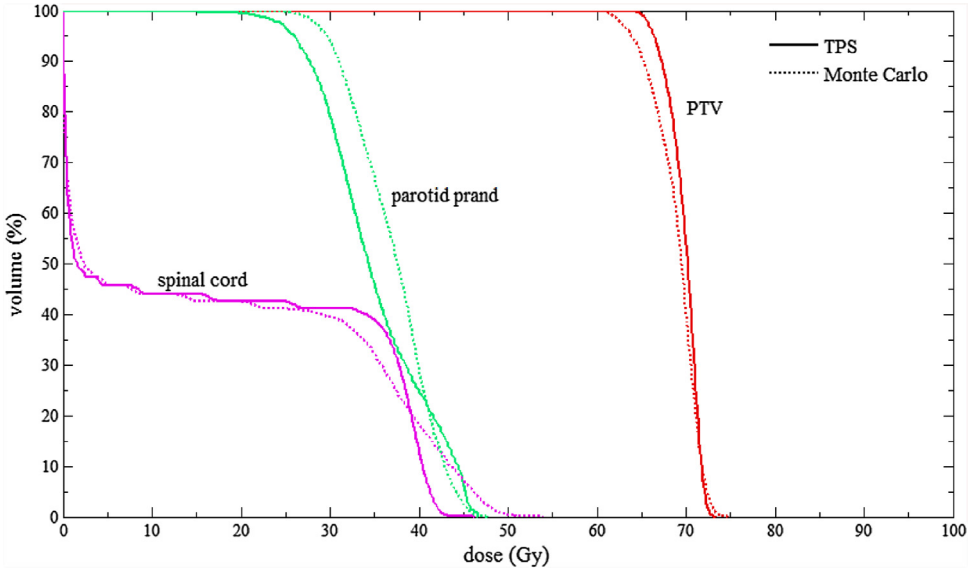

Fig. 13 – The dose volume histograms were calculated by MC and TPS for example treatment.

The differences and agreements between the TPS and MC results can clearly be seen on DVH (Fig. 13). Fig. 13 shows that the dose to the parotid glands and spinal cord were higher than TPS. A plausible explanation for this difference is due in part to electron scattering from the surrounding bone, which could not be modeled properly using the CCC algorithm.[7] The EGSnrc algorithm, on the other hand, permits calculating accurate dose near the border of materials of different density.

6. Conclusions

We implemented the EGSnrc-based Monte Carlo simulation to verify the JO-IMRT plans generated by Prowess Panther TPS using CCC algorithm. Our results show that the CCC algorithm was adequate for most of the IMRT H&N cases where the target was not immediately adjacent to the critical structures.

Conflicts of interest

None declared.

Financial disclosure

None declared.

Acknowledgments

The authors wish to thank Professor. James C.L. Chow, University of Toronto, Ontario, Canada for providing DOSCTP and his contributions. The first author also would like to extend thanks to Professor Parham Alaei, Director of Medical Physics, Department of Radiation Oncology, University of Minnesota and Professor David W.O. Rogers, Physics Department – Carleton University for their revising on the paper.

REFERENCES

1. Earl MA, Afghan MKN, Yu CX, et al. Jaws-only IMRT using direct aperture optimization. *Med Phys* 2007;**34**(1):307–14.
2. Nishimura Y, Komaki R. *Intensity-modulated radiation therapy: clinical evidence and techniques*. Springer; 2015. p. 22–7.
3. John N. Method for intensity modulated radiation treatment using independent collimator jaws. US Patent 2006;7180980.
4. Tai DT, Binh DT, Hai NV, et al. Applied research in technique of intensity modulated radiation therapy (JO-IMRT) in Dongnai General Hospital. *IOSR J Eng* 2014;**4**(2):35–8.
5. Tai DT, Son ND, Loan TTH, et al. Initial experiences of applying the jaws-only IMRT technique in Dong nai general hospital, Vietnam. *IFMBE Proc* 2018;**63**:335–9.
6. Tai DT, Son ND, Loan TTH, et al. Quality assurance of the jaws only-intensity modulated radiation therapy plans for head-and-neck cancer. *Phys Med* 2017;**38**:148–52.
7. Ma CM, Pawlicki T, Jiang SB, et al. Monte Carlo verification of IMRT dose distributions from a commercial treatment planning optimization system. *Phys Med Biol* 2000;**45**(9):2483–95.
8. Ma CM, Mok E, Kapur A, et al. Clinical implementation of a Monte Carlo treatment planning system. *Med Phys* 1999;**26**(10):2133–43.
9. Francescon P, Cora S, Chiovati P. Dose verification of an IMRT treatment planning system with the BEAM EGS4-based Monte Carlo code. *Med Phys* 2003;**30**(2):144–57.
10. Leal A, Sánchez-Doblado F, Arráns R, et al. Routine IMRT verification by means of an automated Monte Carlo simulation system. *Int J Radiat Oncol Biol Phys* 2003;**56**(1):58–68.
11. Pawlicki T, Ma CM. Monte Carlo simulation for MLC-based intensity-modulated radiotherapy. *Med Dosim* 2001;**26**(2):157–68.
12. Sakthi N, Keall P, Mihaylov I, et al. Monte Carlo-based dosimetry of head-and-neck patients treated with SIB-IMRT. *Int J Radiat Oncol Biol Phys* 2006;**64**(3):968–77.
13. Rogers DWO, Walters B, Kawrakow I. BEAMnrc User's manual. NRCC Report PIRS-0509(A)revL.
14. Rogers DWO, Faddegon BA, Ding GX, et al. BEAM: a Monte Carlo code to simulate radiotherapy treatment units. *Med Phys* 1995;**22**(5):503–24.
15. Kawrakow I, Mainegra-Hing E, Rogers DWO, et al. The EGSnrc Code System: Monte Carlo Simulation of Electron and Photon Transport, NRCC Report PIRS-701.
16. Popescu IA, Shaw CP, Zavgorodni SF, et al. Absolute dose calculations for Monte Carlo simulations of radiotherapy beams. *Phys Med Biol* 2005;**50**(14):3375–92.
17. Bergman AM, Bush K, Milette MP, et al. Direct aperture optimization for IMRT using Monte Carlo generated beamlets. *Med Phys* 2006;**33**(10):3666–79.
18. Tai DT, Son ND, Loan TTH, et al. A method for determination of parameters of the initial electron beam hitting the target in linac. *J Phys Conf Ser* 2017:851.
19. Walters B, Kawrakow I, Rogers DWO. DOSXYZnrc User's manual. NRCC Report PIRS-794revB.
20. Chow JCL, Leung MKK. A graphical user interface for calculation of 3D dose distribution using Monte Carlo simulations. *J Phys Conf Ser* 2008;**102**, 0120-03.
21. Chow JCL. Some computer graphical user interfaces in radiation therapy. *World J Radiol* 2016;**8**(3):255–67.
22. Type Chamber FC65-P. Technical description. DFK000 12001 00.
23. Deasy JO, Blanco AI, Clark VH. CERR: a computational environment for radiotherapy research. *Med Phys* 2003;**30**(5):979–85.
24. Navin S, Sunil DS, Nirmal KP, et al. Underdosing of the maxillary sinus for small fields used in newer radiotherapy techniques: Comparison of thermoluminescent dosimeter and Monte Carlo data. *J Can Res Ther* 2018;**14**(2):351–6.
25. Hideharu M, Norihisa M, Kouichi Y, et al. Evaluation and commissioning of commercial Monte Carlo dose algorithm for air cavity. *Int J Radiat Oncol Biol Phys* 2014;**3**(1):9–13.